On the Use of Quartic Force Fields in Variational Calculations

Ryan C. Fortenberry

NASA Ames Research Center, Moffett Field, California 94035-1000, U.S.A.

Xinchuan Huang

SETI Institute, 189 Bernardo Avenue, Suite 100, Mountain View, California 94043, U.S.A.

Andrey Yachmenev*

Max-Planck-Institut für Kohlenforschung, Kaiser-Wilhelm-Platz 1, D-45470 Mulheim an der Ruhr, Germany

Walter Thiel

Max-Planck-Institut für Kohlenforschung, Kaiser-Wilhelm-Platz 1, D-45470 Mulheim an der Ruhr, Germany

Timothy J. Lee**

NASA Ames Research Center, Moffett Field, California 94035-1000, U.S.A.

Abstract

The use of quartic force fields (QFFs) has been shown to be one of the most effective ways to efficiently compute vibrational frequencies for small molecules. In this paper we outline and discuss how the simple-internal or bond-length bond-angle (BLBA) coordinates can be transformed into Morse-cosine(-sine) coordinates which produce potential energy surfaces from QFFs that possess proper limiting behavior and can effectively describe the vibrational (or rovibrational) energy levels of an arbitrary molecular system. We investigate parameter scaling in the Morse coordinate, symmetry considerations, and examples of transformed QFFs making use of the MULTIMODE, TROVE, and VTET variational vibrational methods. Cases are referenced where variational computations coupled with transformed QFFs produce accuracies compared to experiment for fundamental frequencies on the order of 5 cm^{-1} and often as good as 1 cm^{-1}.

Keywords: quartic force fields, morse-cosine coordinates, variational vibrational methods, vibrational configuration interaction theory, vibrational frequencies

1. Introduction

The quartic force field (QFF) is a simple and elegant means by which one can adequately describe the near equilibrium potential surface for a molecular system. A QFF is

*Current addresses: Karlsruher Institut für Technologie, Kaiserstr. 12, 76131 Karlsruhe, Germany
**Corresponding author
Email address: Timothy.J.Lee@nasa.gov (Timothy J. Lee)

simply the fourth-order Taylor series approximation of the anharmonic potential of the form:

$$V = \frac{1}{2}\sum_{ij} F_{ij}\Delta_i\Delta_j + \frac{1}{6}\sum_{ijk} F_{ijk}\Delta_i\Delta_j\Delta_k + \frac{1}{24}\sum_{ijkl} F_{ijkl}\Delta_i\Delta_j\Delta_k\Delta_l \quad (1)$$

with displacements Δ_i and force constants $F_{ij\ldots}$. Methods utilizing QFFs have been shown to provide accuracies often as good as 1 cm^{-1} with experiment and routinely as close as 5 cm^{-1} in describing the fundamental vibrational frequencies for various systems [1–18] though QFFs based on coupled cluster singles, doubles, and perturbative triples [CCSD(T)] [19] energies produce such accuracies partly due to a cancellation of errors in the electronic structure method, as has been discussed [20–22]. Vibrational perturbation theory (VPT) [23–25] at second-order (VPT2) is most often combined with QFFs for determination of rovibrational properties. Much success is reported in the literature for reproducing experimental frequencies and reporting previously unobserved modes [26–33]. These studies and many others showcase how beneficial molecular frequencies computed with QFFs and VPT2 are to the chemistry and physics communities.

There have been some cases, however, that highlight where VPT2 can fail, and these differ from known weaknesses in QFFs. When VPT2 is not a valid choice of vibrational method, other tools must be employed to solve the nuclear Schrödinger equation. For example, Martin and Taylor [34] found that the strongly anharmonic N−H stretching mode in the H_2NN molecule cannot be adequately described with VPT2 but can be using variational procedures. This was consistent with an earlier study that found a similar N−H stretch anharmonicity for the HNO molecule [3]. Further work [35] analyzed the role that variational computations can play in improving the description of anharmonic frequencies and found that non-negligible anharmonic effects in hydrogen peroxide and, to a lesser degree, hydrogen persulfide are not properly accounted for within VPT2. Hence, expansion-style wavefunction-based vibrational methods are sometimes the only means of reliably describing vibrational frequencies beyond the harmonic approximation.

Variational methods for the computation of anharmonic vibrational frequencies can take many forms, and many are connectivity-specific or, in the very least, formulated for a specific number of atoms. Work on tetra-atomic systems increased the amount of chemistry that can be accurately modeled by quantum chemical procedures. In the VTET approach by Schwenke [36] and the DVR(n) methods by Mladenović [37], explicit terms for the kinetic and potential energy terms are derived based on how the atoms interact with one another within a chosen or developed set of vibrational basis functions. Recent work [38–41] has shown how these approaches are beneficial in resolving issues with computed vibrational frequencies.

Other methods and codes, especially those of the newest generation, are designed to be more general and are built around terms that can be applied to systems of an arbitrary number of atoms without regard for the specific connectivity or symmetry. The TROVE program [42] constructs a general vibrational Schrödinger equation and expands the kinetic and potential energy operator terms in the Hamiltonian with polynomials. An active space of vibrational states is chosen to contain the expansion, and the potential energy function (which can be input from QFFs) for certain geometrically defined coordinates completes the Hamiltonian. Diagonalization of the Hamiltonian results in the vibration-rotation energies and wavefunctions, where the latter are the descriptions of the actual molecular behavior. This scheme also gives purely rotational states and mixed

vibration-rotation states. TROVE has been utilized since its development to provide line lists for common systems like NH_3 [43, 44] and even to resolve some of the anharmonicity issues experienced with peroxide-like systems such as HSOH [45, 46].

Another, generally-applicable program designed to treat anharmonic vibrational computations is MULTIMODE (MM) [47–50]. This program makes explicit use of vibrational configuration interaction (VCI) theory in order to describe the rovibrational wavefunction. Within the Hamiltonian, the potential is defined as a hierarchical combination of intrinsic potential terms, $V_i^{(N)}(Q_i)$ for coordinates Q_i. N is the number of modes considered in a single potential term, and the maximum of N leads to the so-called mode-representation (MR) of the total VCI potential. The coupled potential terms produce the VCI potential:

$$V(Q_1, Q_2, \ldots, Q_N) = \sum_i V_i^{(1)}(Q_i) + \sum_{ij} V_{ij}^{(2)}(Q_i, Q_j) + \cdots + \sum_{ijk\ldots N} V_{ijk\ldots N}^{(N)}(Q_i, Q_j, Q_k, \ldots, Q_N). \tag{2}$$

The above VCI potential is then included in the Watson Hamiltonian [51, 24]:

$$H = \frac{1}{2}\sum_{\rho\sigma}(J_\rho - \pi_\rho)\mu_{\rho\sigma}(J_\sigma - \pi_\sigma) - \frac{1}{2}\sum_k \frac{\partial^2}{\partial Q_k^2} - \frac{1}{8}\sum_\rho \mu_{\rho\rho} + V(\mathbf{Q}). \tag{3}$$

J_ρ is the total angular momentum of a given cardinal direction ($x, y,$ or z) denoted by ρ or σ in Eq. 3; π_ρ is the total vibrational angular momentum of the same direction; $\mu_{\rho\sigma}$ is the inverse of the moment of inertia tensor for the given geometric coordinates; and $\mathbf{Q}$ is the set of all normal coordinates. With the potential and Hamiltonian defined, the vibrational self-consistent field (VSCF) equations can be formulated and solved. These, in turn, are fed into the VCI equations. Both sets of equations and their solution steps are discussed in Ref. [48]. In VCI, full-CI is achieved when N or, equivalently, NMR equals the total number of modes the molecule may possess. For a four-atom system, full-CI is 6MR from $3N-6$. Table 1 gives a comparison for MM and TROVE for ammonia where, at the full computational level for each method, the two agree to better than 0.4 cm^{-1} for every frequency.

However, all of these post-harmonic, non-VPT2, variational methods require the input of a potential function. QFFs often reliably describe the potential near equilibrium. Global or semi-global surfaces are useful, as well, but they are much more computationally costly in the formulation of the potential. However, the larger expansions of the variational wavefunctions routinely require states where bond length-bond angle (BLBA) or simple-internal coordinates are known to break-down when QFFs are used to define the potential. Hence, in order for these methods to be effective, they must have what is called "correct limiting behavior."

2. Transforming to a Morse-Cosine Coordinate System

2.1. Correct Limiting Behavior

In simple-internal or BLBA coordinates, QFFs are known to produce non-physical results when attempting to describe behavior at distances just beyond the equilibrium geometry and at values larger than the QFF displacements [52–54]. This is especially

true for the bond lengths where the energy, depending on the case, can either grow continually toward positive infinity as the bond length is stretched [3], or turn over and deteriorate below the minimum and continue toward negative infinity as other formulations of coordinates have been shown to do [55–57]. For the case of the O−H stretch in water, shown in Fig. 1, the BLBA coordinate QFF, denoted by the black curve, exhibits the unchecked increase toward positive infinity. This is also present in the N−H and C−H stretches for ammonia and methane in Figs. 2 and 3. Hence, the resulting variational wavefunction becomes incapable of describing behavior for distances anything more than slightly larger than the equilibrium bond lengths. If the reference geometry is not close to the actual potential minimum or if the artificial barrier for a turnover to negative infinity is not tall or wide enough, this problem can be more pronounced, depending on the variational method.

For bond stretches, the Morse potential converges to an asymptotic limit where the atoms become noninteracting. In order for a potential energy surface (PES) to possess "correct limiting behavior," the energies of the displacements for longer bond lengths must converge to some value in a similar way. This does not have to be the actual Morse potential limit even though such would definitely be the desired case, but the PES must have a similar shape. The incorrect limiting behavior of the PES given by a QFF along a bond length coordinate can be easily rectified by transforming the QFF into a coordinate system in which correct limiting behavior is conserved.

An easily understood transformation of coordinates to address PES and QFF correct limiting behavior was brought forth by Simons, Parr, and Finlan (SPF) [57] originally for diatomic molecules. In these coordinates, R, the equilibrium bond length, r_e, is used to modify the displaced bond length, r, in the form:

$$R = \frac{r - r_e}{r}. \tag{4}$$

These SPF coordinates often prohibit the potential from turning over towards negative infinity as the related Dunham [55, 56] or simple BLBA coordinates are known to do. In SPF coordinates, r replaces r_e as the denominator from their Dunham counterparts. SPF coordinates do not directly model the Morse-like behavior at longer bond lengths [57]. In fact, they often diverge noticeably from the Morse-potential shortly beyond the equilibrium geometry and are not guaranteed to converge to any limit. The difference between SPF coordinate-based energies and the Morse limits is great enough that at large enough bond lengths, highly non-physical behaviors are modeled, but this is not as great as is often observed in BLBA coordinates that may approach positive infinity much faster [57, 3]. Hence, SPF coordinates often will not give correct limiting behavior but do so in quite a different manner as compared to Dunham or BLBA representations. That being said, SPF coordinates can force the weighting of the wavefunction towards the actual bottom of the well overcoming one issue with coordinates without correct limiting behavior. As a result, computations that require longer bond lengths in the potential are possible with SPF coordinates, but they are not as robust as would be desired.

2.2. Form of the Morse Coordinate

Other formulations of coordinates attempt to rectify the issues that SPF cannot. Watson [51] proposed a means of describing bond lengths with Morse-like behavior even before SPF coordinates were introduced. However, it was not until Meyer, Botschwina,

and Burton [58] popularized this approach, followed shortly by Carter and Handy [59], that it began to gain acceptance. These new coordinates, R, are Morse-like and are defined [58] as:

$$R = \frac{1 - e^{-\beta(\frac{r}{r_e}-1)}}{\beta} \tag{5}$$

where β is a parameter that can be optimized for the system of interest. It is this style of bond length coordinate that has been applied most straightfowardly to QFFs for use in describing the anharmonic potential for variational computations.

Later, a different but related formulation of the Morse-like coordinates was suggested by Dateo, Lee, and Schwenke [3]:

$$R = 1 - e^{-\alpha_r(r-r_e)} \tag{6}$$

where α_r is again an optimizable parameter that can vary for each bond length present in the computation. The general parameter, α_i, was defined as:

$$\alpha_i = -\frac{f_{iii}}{3f_{ii}} \tag{7}$$

where these diagonal elements of the three- and two-body force constant matrices are still in internal coordinates and have not yet been transformed. Such a definition of the α parameter forces the transformed force constant, F_{iii}, to be zero. Unlike Eq. 5, Eq. 6 does not include the parameter as the denominator term in its formulation, but this still leaves the equation with convergence to some limit and is nearly the exact form as the Morse potential itself, mostly by design. Even so, coordinates defined either by Eq. 5 or Eq. 6 will behave similarly though they converge to slightly different limits. Hence, both have correct limiting behavior at least in a semi-quantitative sense. The red curves in Figs. 1-3 showcase how Morse-type coordinates (as defined by Eq. 6) differ from BLBA coordinates, especially as the bond length is increased. The inflection points as the red curves trend toward a limit can be observed. As a result, Morse coordinates for bond stretching modes are essential when using QFFs together with variational anharmonic vibrational calculations.

2.3. Cosine for Simple Bending Angle Coordinates

It is not just the bond lengths that need modification, however. Methods like VCI in MULTIMODE allow the modes to couple together within the potential and are further susceptible to inaccuracies in the PES brought about by the descriptions of the modes from the chosen coordinate type. Potential curves along a single bond angle must be periodic in nature. However, BLBA coordinates may overshoot the vibrational energy at various points on the potential, especially for values close to π [3]. These non-physical descriptions using BLBA coordinates can also be overcome with transformations which need not be exceptionally complicated. The standard bond angle displacement coordinate, termed the theta coordinate, is defined below:

$$\Theta = \theta - \theta_e. \tag{8}$$

Coupled with Morse coordinates for the stretches, this coordinate system is denoted Morse-theta.

However, as indicated, it is often necessary to have the potential exhibit periodic behavior, and this may be achieved by taking the cosine of each angle:

$$\Theta = \cos(\theta) - \cos(\theta_e). \tag{9}$$

The use of Morse coordinates and these cosine transformed bond angle coordinates as a set is referred to as Morse-cosine coordinates. QFFs in this coordinate system have been previously shown to produce highly accurate frequencies when coupled with variational computations [3, 6, 9, 10, 12–18]. As an example, the QFF-based fundamental frequencies for ammonia have been computed with the VTET program using both Morse-cosine and Morse-theta coordinates. These are given in Table 1. For the bond stretching frequencies, the change in the bend coordinate has an effect of a negligible 0.15 cm^{-1} or less, but the change between Morse-cosine and Morse-theta coordinates is a noticeable 1.7 cm^{-1} or more for the bending modes. Furthermore, Fig. 4 shows the difference in behavior between the theta bond angle coordinate in black and the cosine coordinate in red for water. For this triatomic molecule, the major difference in the two is at π where the theta coordinate overshoots the energy and can introduce errors in the vibrational calculation.

Lastly, close examination of the results in Table 1 shows that even though only a QFF was used for ammonia, the variational treatment for solving the nuclear Schrödinger equation leads to a symmetric double-well potential, and hence the inversion splitting of all energy levels, which is a hallmark for the ammonia molecule. (The reader should note that for the E modes, we report different parities due to the inversion splitting, and hence they are not identical.) In fact, comparison of the various splitting values between the QFF results, whether from TROVE or VTET, with the values obtained from a highly accurate global PES, HSL2 [39, 40], shows that they are in remarkably good agreement. The inversion splitting values obtained using the MULTIMODE program are still reasonably good, but not as accurate as obtained with VTET and TROVE. In this case, the ammonia QFF used in the variational calculations has an inversion barrier of 1778 cm^{-1} versus 1785 cm^{-1} for the HSL2 global PES.

2.4. The Choice of Alpha

Since the α value in the Morse coordinate of Eq. 6 is an arbitrary parameter, this value can be calibrated to give different results. As such, α can be chosen to exactly describe the dissociation limit determined from high-accuracy theoretical or experimental data. For cases where such data is not known or cannot be determined, a standard and accurate definition of α is valuable. Dateo, Lee, and Schwenke [3] proposed the definition of α given above in Eq. 7, but this choice of α has not been systematically studied for its performance in computations of the vibrational frequencies with Morse coordinates. Tables 2-4 highlight how changes in the α parameter affect the frequency computed for the fundamentals of NH_3, H_2O, and CH_4, respectively.

One obvious choice of α would be the one that gives the proper dissociation energy (D_e). The computed D_e for each QFF of a given molecule, as listed in Tables 2-4, is the asymptotic limit that the potential surface approaches as r increases toward positive infinity. These D_e values are computed from relaxed optimizations which means they allow the other bonds to respond and reach a local minimum energy geometry as the principle bond is stretched. When scaling the computed D_e with regards to the experimental D_e,

it is shown that the standard (Eq. 7) choice of α performs quite well in describing the dissociation energy. A $\pm 5\%$ range for the Eq. 7 choice in α contains the experimental D_e for our three test cases. The results for α are within 3.5% of the experimental values for ammonia, 1.84% for water, and 2.45% for methane. Water would need a smaller α to match the experimental D_e while ammonia and methane would need a larger α value to do so.

In Table 2, the ammonia fundamental vibrational frequencies are computed with TROVE. The QFF used is fitted from energies determined from within the HSL2 global PES [39, 40] at individual displacements of 0.005 Å for the bond lengths and 0.005 radians for the bond angles and is transformed into the Morse-theta coordinate system. The fundamental vibrational frequencies computed are within 4.5 cm^{-1} or better with the spectroscopically accurate HSL2 results. Furthermore, a variance of $\pm 5\%$ from the standard α value computed by way of Eq. 7 changes the stretching frequencies by only 1.24 cm^{-1} and 1.61 cm^{-1}. The degenerate deformation bends are affected by 0.07 cm^{-1} or less. These results indicate that the value of α is well-behaved for the definition given in Eq. 7. Compared with the HSL2 results for the fundamentals in Ref. [39, 40], many of the modes, such as ν_2 and ${\nu_3}^{\pm}$, could benefit from a decrease in the α parameter. Others, like ${\nu_4}^{\pm}$ compare nicely for the unscaled α in the "1.0" column of Table 2. Regardless, this choice of α created without any assumption or experimental data input is able to give correct limiting behavior whose asymptotic limit is very close to the experimental D_e, and also is an integral part in the generation of fundamental frequencies to fairly high accuracy.

The behavior of the frequencies for water and methane with MM VCI using Morse-cosine coordinates in Tables 3 and 4 is similar to the ammonia results computed with TROVE. However, the fundamentals for water are computed with the cC QFF from Ref. [9]. The latter QFF is so named here with the convention utilized later [13, 18] since it is defined from CCSD(T) [19] (described above) utilizing aug-cc-pCVTZ, aug-cc-pCVQZ, and aug-cc-pCV5Z basis sets [60–62] extrapolated to the complete basis set (CBS) limit with a three-point formula [63]. The so-called LMT QFF used for the methane computations is from Ref. [4] and is defined from CCSD(T)/cc-pVQZ energies at points defined from displacements like those in ammonia.

From Tables 3 and 4 it can be seen that the fundamentals for water differ from experiment by less than 2.5 cm^{-1} and differ by less than 4 cm^{-1} for methane. The variance between frequencies for values of α within the $\pm 5\%$ range for water and methane are on the order of 0.1 cm^{-1} for the angle bends and less than 2.0 cm^{-1} for the bond stretches. While ammonia and water have many modes that would benefit slightly from a decrease in the choice of α, many modes of methane would perform better with an increase in α. Further, there are several modes for these three test cases where the frequencies compare favorably with experiment for the Eq. 7 choice of α. Hence, the current choice of α, which does not require any prior knowledge of the system analyzed, can give reliable fundamental vibrational frequencies provided the QFF is also accurate.

The differences in the α values are visually depicted in Figs. 1-3 where the blue, red, and green curves correspond to 0.7, 1.0 (unscaled), and 1.3 α scalings for the X−H stretches in water, ammonia, and methane, respectively. The three different colored curves in each figure begin to diverge a few tenths of an Ångstrom beyond the equilibrium bond length. The blue 0.7 α potential curves are higher in energy than the standard red curve beyond the divergence point, and the 1.3 α green curves are lower in energy. This

behavior is expected from the negative exponential definition of the Morse coordinate in Eq. 6. Not only does the choice of α defined in Eq. 7 readily produce accurate fundamental frequencies, it also yields results for the D_e values that are very close to the experimental quantity and, as a result, correct limiting behavior for systems for which experimental data is not available.

2.5. More Complicated Structures

There are occasions where simple Morse-cosine transformed coordinates for a QFF are not adequate to treat a system. Two examples are planar, cyclic structures and linear structures. In cases where the equilibrium bond angle coordinate value is close to 0 or π, sine coordinates of the form:

$$\Theta = \sin(\theta) - \sin(\theta_e) \tag{10}$$

are necessary. In the fitting of the force constants, derivatives of the coordinates appear in denominator terms. At the equilibrium geometry of a linear structure, for instance, $\frac{d}{d\theta}\cos(\pi) = -\sin(\pi) = 0$. Hence, a non-zero gradient term is necessary to avoid an infinity value arising from a 0 in the denominator. Usage of these coordinates in conjunction with cosine coordinates for the other angles with bonds that are greater than 0 and less than π leads to the so-called Morse-cosine-sine coordinates. The usage of these coordinates has been shown to be valuable in linear $C_{\infty v}$ molecules like CCH^- [10] where the sine coordinate is necessary to accurately treat the Π bending mode.

Furthermore, the high levels of redundancy for some coordinates, like the C−C bonds within benzene together with the C−C−C bends, can create havoc when manipulating QFFs. As a result, symmetry adaptation of the simple internal coordinates must be used in highly symmetric structures before construction of the QFF and transformation to Morse-cosine(-sine) coordinates. Symmetry adaptation has been utilized for highly symmetric structures for some time now [1, 4, 64–66]. Further, recent work on c-$C_3H_3^+$ [12] exemplifies the need for symmetry-adaptation in the coordinate system for a Morse-type coordinate, as well. The initial QFF is constructed in terms of symmetry-adapted internal coordinates making full use of the D_{3h} point group symmetry. For example, complete treatment of the C−C bond lengths becomes a single term, $S_1 = (R_1 + R_2 + R_3)/\sqrt{3}$, since there is a redundancy between the three C−C bond lengths and the three C−C−C bends. A full listing of these coordinates is given in Ref. [12], and all are linear combinations of the redundant set of bond lengths, bond angles, and out-of-plane bends, where the latter are defined as the motion of one hydrogen atom relative to the carbon ring. Usually, the symmetry internal coordinate QFF is transformed directly into the Morse-cosine coordinate system using the definitions in Eqs. 6 and 9. However, in the case of c-$C_3H_3^+$, it is necessary to use a symmetry adapted set of Morse-cosine-sine coordinates due to the redundancy between the C−C bonds and the C−C−C bends. In this case, one can derive formulae to directly transform the symmetry internal coordinate QFF into a symmetry adapted Morse-cosine-sine coordinate QFF, or what was done in Ref. [12] was to re-fit the QFF using the original displacement energies represented in the symmetry adapted Morse-cosine-sine coordinate system. In this way, the new symmetry adapted Morse-cosine-sine QFF has proper limiting behavior, and it also has exact D_{3h} symmetry.

3. Degenerate Vibrational Modes

Generally, VPT2 computations can treat degenerate vibrational modes exactly as long as the QFF is properly constructed in terms of the symmetry coordinates, and this has been done many times (*e.g.* Refs. [1, 4]). However, for variational vibrational calculations the proper treatment of degenerate vibrational frequencies is more complicated. Different variational vibrational methods treat symmetry in different ways. This is mainly a response to the formulation of the method itself and how the symmetry relationships fit within the equations. For those methods that are general, especially with regards to the number of possible atoms included in the computation, the symmetry treatment must be generalized in some fashion as similar to electronic structure computations [67].

However, neither variational vibrational nor electronic structure codes are regularly coded to treat symmetries of point groups beyond D_{2h} and its subgroups. D_{2h} and its subgroups all possess purely one-dimensional irreducible representations (irreps) which give straightforward mathematical relationships to be coded. Hence, degenerate vibrational modes may not be properly treated. As a result, linear combinations of lower symmetry irreps must be employed to describe the degenerate modes of higher symmetries. In the MULTIMODE VCI program, C_{2v} and its subgroups, C_s and C_2, can be treated. Higher-order point group molecules can also be included, but they must use the largest Abelian subgroup available. As a result of this lack of explicit symmetry treatment, there are three different ways in which inadequate treatment of degenerate modes in higher-order symmetries can be introduced: the Hamiltonian, the wavefunction, and the basis size, or, in other words, inadequate convergence thresholds.

3.1. The Hamiltonian

In order to maintain symmetry, the Hamiltonian must be exact or approximated in such a way that components of a degenerate vibrational mode are treated in the same way [24, 68]. An example of where this problem was identified in an electronic structure method is given in Ref. [69] for the OPT2, open-shell perturbation theory, method. For the vibrational problem, when considering systems of high symmetry, there can exist errors in the formulation of the kinetic energy terms for point groups with multidimensional irreps if care is not taken when approximating the kinetic energy operator. Most notably, however, the QFF (the potential term in the Hamiltonian) may be easily forced to properly treat the symmetry relationships of the system. This was shown in a few early cases [1, 4, 64], and QFF symmetry relationships have now been published for molecules of the form X_3 (D_{3h}) [65], X_4 (T_d) [65], XY_3 (C_{3v}) [70, 1, 27], XY_3 (D_{3h}) [71, 7], XY_4 (T_d) [4, 64], XYZ ($C_{\infty v}$) [72, 73, 2], XY_2 ($D_{\infty h}$) [72, 71], X_2Y_2 ($D_{\infty h}$) [74, 72, 75], and X_3Y_3 (D_{3h}) [12].

3.2. The Wavefunction

The second consideration of symmetry is from the wavefunction perspective. The symmetry modes for MULTIMODE are defined by the user in the input. The MM VCI potential (Eq. 2) must be totally symmetric since the Hamiltonian, by definition, is totally symmetric [76], and the QFF terms must be also. Hence, the different irrep-labeled mode interrelation to mimic higher-symmetry is already defined when the potential (Eq. 2) is created. This forces the wavefunctions themselves to describe the desired symmetry states. The TROVE program operates in a similar fashion. The explicit degeneracies

present in the higher symmetry can be lost when the irreps are transformed to lower symmetry. Degenerate states are comprised of linear combinations of various irreps. As a result, certain pieces of the necessary linear combination may be discarded if those states are above a certain inclusion threshold. Hence, more terms in the VCI expansions and more basis functions per irrep are typically necessary to fully describe the actual degeneracies. Within a 3, 4, or 5MR VCI computation, a degenerate pair of vibrational modes may not be fully contained within the wavefunction since all combinations of three, four, and five modes are included in the highest substitution level of the wavefunction terms where other terms, including the degenerate partner, may be excluded. Hence, higher substitution levels in the CI wavefunction allow for a more complete description of the vibrational wavefunction. At the full CI level, all of the possible excited states in the wavefunction are included and degenerate levels will be described properly, but only a few interesting molecules can be computed at this level.

Table 5 highlights how larger numbers of terms in the wavefunction improve the variational computation of the frequencies for degenerate modes. For the 4MR ν_3 frequencies of ammonia computed with MULTIMODE, the ν_3^+ and ν_3^- values differ by 23.92 cm^{-1}. However, simply increasing the number of virtual states included in the wavefunction by using 5MR decreases this difference by two orders of magnitude to 0.59 cm^{-1}. 6MR is of course full CI for ammonia, and the differences between the 5MR and 6MR results are small. As discussed previously, the E modes for ammonia do not come out exactly degenerate because different parities of the inversion split energy levels are reported.

The degenerate modes of methane, given in Table 6, show a better case for the use of larger expansions in the VCI wavefunction. The doubly degenerate ν_2 frequencies differ by 0.20 cm^{-1} for 3MR, 0.02 cm^{-1} for 4MR, and are degenerate to better than 0.01 cm^{-1} for 5MR. The ν_4 degenerate frequencies behave similarly as the components for ν_2. The ν_3 frequencies differ by only 0.13 cm^{-1} for the 5MR computations, while the 3MR frequencies are in disagreement by 8.95 cm^{-1}. BH_3 (given in Table 7) also shows improvement for the higher substitution level in the VCI wavefunction. The QFF defined from the CBS extrapolated energy refined for non-Born-Oppenheimer and scalar relativisitic effects (CBR) has already been employed with VPT2 [7] with high accuracy. Using the same QFF, the degenerate E' ν_3 mode components of BH_3 are nearly exactly degenerate at the 5MR level, while the other E' mode, ν_4, varies between the computed energy levels by less than 0.01 cm^{-1}. Hence, increasing the size of the wavefunction will improve the description of the degenerate modes such that discrepancies between the two or more computed components in a system with a single-well minimum can agree to better than 0.01 cm^{-1}.

3.3. Convergence Thresholds

The issue with energy-level degeneracies computed with lower symmetries also requires the use of very tight convergence criteria in the vibrational wavefunction. This approach has been proven effective for electronic structure computations [69]. Tighter convergence thresholds must also be applied to the construction of the wavefunctions in the rovibrational computations. Work on the cyclic (D_{3h}) form of $C_3H_3^+$ [12] has showcased the reliability in using QFFs and C_{2v}-based VCI to describe the rovibrational properties of a highly symmetric system. BH_3 in Table 7 also shows how larger basis sets can improve the agreement in degenerate components, where the ν_4 components of

1196.6889 and 1196.6936 cm^{-1} shrink the 0.0053 cm^{-1} gap to 0.0012 cm^{-1} with frequencies of 1196.6059 cm^{-1} and 1196.6071 cm^{-1}. This demonstrates that the size of the underlying basis set is important for convergence of computed energy levels and maintaining the symmetry of different components of a degenerate mode.

4. Combination Bands, Overtones, and Higher-Energy States

As previously mentioned, variational vibrational approaches making use of Morse-cosine QFFs have been able to produce accuracies for fundamental vibrational frequencies of routinely 5 cm^{-1} and as close as 1 cm^{-1} in some cases [3, 6, 9, 10, 12–18]. However, comparative data for the overtones and combination bands is not as common. The overtones and combination bands are often much less intense and of less significance in the analysis of experimental vibrational spectra. However, they can play a defining role in the spectra of certain systems, especially smaller molecules with fewer fundamental vibrational frequencies.

If correct limiting behavior and proper coordinates are necessary for the fundamental vibrational frequencies, they are more important for the combination bands and overtones. This should be apparent since the energy levels for combination and overtone bands will be higher up the potential well. However, examination of the VPT2 term value expression shows that even harmonic frequency errors are magnified for higher energy levels [24, 25], and this will be apparent in variational calculations of vibrational energy levels, as well. In the following section we compare the transition energy for VCI combination and overtone bands relative to experiment for the water molecule (using the aforementioned Morse-cosine cC QFF), followed by a comparison of the VCI and VPT2 results.

4.1. Comparison of VCI with Experiment

As an example, several theoretical (cC 3MR VCI MULTIMODE) and experimental (Ref. [77]) fundamental vibrational frequencies, overtones, and combination bands of water are listed in Table 8. Since water only has three degrees-of-freedom, 3MR is full-CI. The cC VCI fundamentals differ from the corresponding experimental frequencies by an average of 4.08 cm^{-1}. As a result, some of this difference gets compounded in the overtones, especially for the ν_2 bending frequency. The state with the most difference in the computed result as compared to experiment is the 4649.42 cm^{-1} $3\nu_2$ overtone which is 17.37 cm^{-1} lower than the 4666.790 cm^{-1} experimental result. The next-largest experimental difference is 8.31 cm^{-1} from $2\nu_2$, which is an overtone of the same mode. On the opposite end of the error spectrum, the $\nu_1+\nu_2$ combination band exhibits the smallest theoretical difference from experiment, 1.85 cm^{-1}. These examples appear to indicate some level of compounding or cancellation of the error as will occur with combination and overtone bands

The VCI overtones and combination bands will compound or cancel the errors some, but only to a certain degree as appears in the above cases. However, whether the error compounds or is canceled to some extent for a higher-lying vibrational state is difficult to predict in advance since errors in the harmonic part of the calculation may be different (and the opposite sign) to those for the anharmonic part. To illustrate, even though the computed 3661.86 cm^{-1} ν_1 differs from experiment by 4.81 cm^{-1}, the computed 7205.20

cm^{-1} $2\nu_1$ differs from experiment by only 3.66 cm^{-1}, and $3\nu_1$ differs by an even less 3.30 cm^{-1}. Moreover, $\nu_1 + \nu_3$ has an error of 2.15 cm^{-1} from experiment. This is less than half of what the error is for either of the stretching fundamentals. In both of these cases, errors for the combination and overtone bands were smaller than for the fundamentals, showing a cancelation of errors for the higher-lying states.

The average difference from experiment for the overtones included in Table 8 is only 4.97 cm^{-1}. Furthermore, besides those frequencies involving overtones of ν_2, no state differs from experiment by more than 5.0 cm^{-1} with an average error of 3.12 cm^{-1}. Thus, the VCI results in Table 8 show that a QFF transformed into a Morse-cosine coordinate system can yield accurate vibrational frequencies for combination and overtone bands, though the results for $2\nu_2$ and, especially, $3\nu_2$ suggest that caution should be exercised in evaluating the results.

4.2. Comparison of VCI and Experiment with 2nd Order Perturbation Theory

For tightly bound molecules, most fundamental vibrational frequencies show strong correlation between VPT2 computed with SPECTRO [78] and VCI/QFF computed with MULTIMODE with differences in the frequencies most often less than 5 cm^{-1}. Even so, there are many exceptions to this rule as has been shown in the work on the conformers of the HOCO radical [13, 14] where the VPT2 and VCI torsional modes differ by more than 25 cm^{-1}. (It has been shown that VPT2 is fortuitously more reliable in its computation of this mode as compared to DVR(6) [41].) However, for tightly-bound molecules, examples like this almost always are a result of the molecule possessing a large-amplitude motion, and that is the case here. Similar situations have been reported for NH_3, HNO, and H_2NN, as discussed earlier.

In looking at Table 8, it would appear that VPT2 performs slightly better in the description of the fundamental vibrational frequencies than VCI where both methods make use of the cC QFF [9]. VPT2 is nearly exact for ν_2, but the 1591.96 cm^{-1} VCI frequency is only 2.82 cm^{-1} less than experiment. VPT2 reports the ZPE to be 4662.72 cm^{-1} while VCI is much lower at 4644.68 cm^{-1}, nearly a factor of four closer to the experimentally inferred 4638.39 cm^{-1} ZPE. For ν_1, VCI and VPT2 are within 1.0 cm^{-1} of each other with VPT2 only 0.67 cm^{-1} higher. As a result, VCI is slightly closer to the experimental ν_1 frequency at 3657.04 cm^{-1}. Finally, VPT2 and VCI are nearly coincident for their computation of the ν_3 antisymmetric stretch, and are less than 5.0 cm^{-1} higher than experiment. The average error compared to experiment for the three fundamentals of water computed with VPT2 is 3.56 cm^{-1}, less than 4.08 cm^{-1} with VCI. Closer inspection reveals that VPT2 does a slightly better job describing the bending frequency than VCI, but does not perform as well as VCI for the two stretching modes.

This trend continues for the overtones, combination bands, and higher-energy states. The ν_2 mode and its overtones are better described with VPT2 than they are with VCI, but the difference between VPT2 and experiment is consistently greater than the difference between VCI and experiment for all of the other modes. The average error for VPT2 for all of the states given in Table 8, including the fundamentals, is 12.14 cm^{-1}, 7.27 cm^{-1} higher than that from VCI. The maximum VPT2 difference from experiment is 38.32 cm^{-1} above the experimental 8761.582 cm^{-1} $2\nu_1 + \nu_2$ frequency while the next-largest error is 36.29 cm^{-1} for $2\nu_1$. Hence, it is essential to use methods beyond VPT2 when computing overtones, combination bands, and higher-energy states, and VCI cou-

pled with a QFF transformed into a Morse-cosine coordinate system appears to be a viable alternative.

5. Conclusions

Procedures to utilize QFFs in MULTIMODE or other variational approaches like those found in TROVE or VTET have been under-appreciated even though they have existed for many years [51] and have been utilized for decades [58, 59]. In this work we have shown how QFFs can be used effectively in the computation of vibrational frequencies even with variational methods.

In order to achieve correct limiting behavior in QFFs, the coordinates must be transformed into some scheme that properly describes the energy beyond the vicinity of the potential energy minimum. For bond lengths, this is a modified form of the Morse potential which allows for asymptotic convergence to some dissociation limit. The limit varies with the value of the scaling parameter, α, but the experimental result is contained with a $\pm 5\%$ deviation of the α value defined in a general form nearly twenty years ago [3] (Eq. 6). Additionally, a $\pm 5\%$ deviation from the standard alpha is shown to contain the exact experimental frequency for a given fundamental from our sample set of ammonia, water, and methane. The bond angles also need to be transformed in order to describe properly the potential at values approaching and surpassing π. This transformation is especially important when the bond angle, or a similar coordinate like a torsion, displays some periodic behavior. The most effective means to treat bond angles is through the use of a cosine coordinate (Eq. 9), but some cases, such as high symmetries or specific out-of-plane bends, require the use of the related sine coordinate (Eq. 10).

Symmetry considerations are often necessary in defining the QFF and utilizing them with variational methods. For high symmetry cases (*i.e.*, where there are degenerate vibrational frequencies), the potential (*i.e.*, the QFF), even in the Morse-cosine(-sine) coordinate system, can be forced to obey symmetry constraints such that appropriate degeneracies are exact. Such symmetry relationships amongst the QFF force constants have been derived and published for a whole host of molecules. Thus, the main source of loss of exact degeneracy in a variational vibrational calculation is due either to the variational method treating the components of a degenerate mode differently (as can happen with VCI if less than a full CI is used) or simply due to a lack of convergence. In both cases, these sources of error can be overcome with a large enough calculation.

When using the same QFF, variational methods like VCI are often coincident with VPT2 in computing the fundamental vibrational frequencies. A few exceptions have been noted where VPT2 performs better than VCI [41], but this has only been shown as a better correlation between VPT2 and DVR(6), which is explicitly coded to treat tetra-atomics. VCI often produces frequencies just as close or closer to experiment than VPT2 as shown here and previously [12, 13, 16, 17]. For overtones and combination bands, VCI generally provides a more complete description of the state wavefunction and and a more accurate frequency than the simple perturbational approach in VPT2. For water, the average difference from experiment in the VCI computation of the fundamentals, overtones, and combination bands is less than 5 cm^{-1} while the average error for VPT2 is more than 12 cm^{-1}.

In summary, the use of QFFs in conjunction with variational computations is a valid means by which one may study vibrational or rovibrational frequencies provided the QFF

is transformed into an appropriate coordinate system. QFFs require relatively few points to create a potential surface while sacrificing little in terms of accuracy. This reduces the total computational cost while still producing meaningful results. With the growth of generalized variational vibrational codes, the use of Morse-cosine transformed QFFs allows for various systems to be examined that would be too costly otherwise.

6. Acknowledgements

The authors gratefully acknowledge support from NASA grants 08-APRA08-0050 and 10-APRA10-0167 as well as NASA's Laboratory Astrophysics 'Carbon in the Galaxy' Consortium Grant (NNH10ZDA001N). RCF is funded by the NASA Postdoctoral Program administered through Oak Ridge Associated Universities. XH acknowledges financial support by NASA/SETI Institute Cooperative Agreements NNX09AI49A and NNX12AG96A.

References

[1] J. M. L. Martin, T. J. Lee, P. R. Taylor, An accurate ab initio quartic force field for ammonia, J. Chem. Phys. 97 (1992) 8361–8371.
[2] T. J. Lee, C. E. Dateo, B. Gazdy, J. M. Bowman, Accurate quartic force fields and vibrational frequencies for HCN and HNC, J. Phys. Chem. 97 (1993) 8937–8943.
[3] C. E. Dateo, T. J. Lee, D. W. Schwenke, An accurate quartic force-field and vibrational frequencies for HNO and DNO, J. Chem. Phys. 101 (7) (1994) 5853–5859.
[4] T. J. Lee, J. M. L. Martin, P. R. Taylor, An accurate *ab initio* quartic force field and vibrational frequencies for CH_4 and its isotopomers, J. Chem. Phys. 102 (1) (1995) 254–261.
[5] J. M. L. Martin, T. J. Lee, P. R. Taylor, J.-P. François, The anharmonic force field of ethylene, C_2H_4, by means of accurate *ab initio* calculations, J. Chem. Phys. 103 (7) (1995) 2589–2602.
[6] K. Yagi, K. Hirao, T. Taketsugu, M. W. Schmidt, M. S. Gordon, *Ab initio* vibrational state calculations with a quartic force field: Applications to H_2CO, C_2H_4, CH_3OH, CH_3CCH, and C_6H_6, J. Chem. Phys. 121 (3) (2004) 1383–1389.
[7] M. S. Schuurman, W. D. Allen, H. F. Schaefer III, The *ab initio* limit quartic force field of BH_3, J. Comput. Chem. 26 (2005) 1106–1112.
[8] S. E. Wheeler, Y. Yamaguchi, H. F. Schaefer III, Protonated carbonyl sulfide: Prospects for the spectroscopic observation of the elusive $HSCO^+$ isomer, J. Chem. Phys. 124 (2006) 044322.
[9] X. Huang, T. J. Lee, A procedure for computing accurate *ab initio* quartic force fields: Application to $HO_2{}^+$ and H_2O, J. Chem. Phys. 129 (2008) 044312.
[10] X. Huang, T. J. Lee, Accurate *ab initio* quartic force fields for $NH_2{}^-$ and CCH^- and rovibrational spectroscopic constants for their isotopologs, J. Chem. Phys. 131 (2009) 104301.
[11] A. C. Simmonett, H. F. Schaefer III, W. D. Allen, Enthalpy of formation and anharmonic force eld of diacetylene, J. Chem. Phys. 130 (4) (2009) 044301.
[12] X. Huang, P. R. Taylor, T. J. Lee, Highly accurate quartic force field, vibrational frequencies, and spectroscopic constants for cyclic and linear $C_3H_3{}^+$, J. Phys. Chem. A 115 (2011) 5005–5016.
[13] R. C. Fortenberry, X. Huang, J. S. Francisco, T. D. Crawford, T. J. Lee, The *trans*-HOCO radical: fundamental vibrational frequencies, quartic force fields, and spectroscopic constants, J. Chem. Phys. 135 (2011) 134301.
[14] R. C. Fortenberry, X. Huang, J. S. Francisco, T. D. Crawford, T. J. Lee, Vibrational frequencies and spectroscopic constants from quartic force fields for *cis*-HOCO: The radical and the anion, J. Chem. Phys. 135 (2011) 214303.
[15] N. Inostroza, X. Huang, T. J. Lee, Accurate *ab initio* quartic force fields of cyclic and bent HC_2N isomers, J. Chem. Phys. 135 (2011) 244310.
[16] R. C. Fortenberry, X. Huang, J. S. Francisco, T. D. Crawford, T. J. Lee, Quartic force field predictions of the fundamental vibrational frequencies and spectroscopic constants of the cations $HOCO^+$ and $DOCO^+$, J. Chem. Phys. 136 (2012) 234309.

[17] R. C. Fortenberry, X. Huang, J. S. Francisco, T. D. Crawford, T. J. Lee, Fundamental vibrational frequencies and spectroscopic constants of $HOCS^+$, $HSCO^+$, and isotopologues via quartic force fields, J. Phys. Chem. A. 116 (2012) 9582–9590.
[18] R. C. Fortenberry, X. Huang, T. D. Crawford, T. J. Lee, The 1 $^3A'$ HCN and 1 $^3A'$ HCO^+ vibrational frequencies and spectroscopic constants from quartic force fields, J. Phys. Chem. A. *in press*.
[19] K. Raghavachari, G. W. Trucks, J. A. Pople, M. Head-Gordon, A fifth-order perturbation comparison of electron correlation theories, Chem. Phys. Lett. 157 (1989) 479–483.
[20] J. F. Stanton, Why CCSD(T) works: A different perspective, Chem. Phys. Lett. 281 (1997) 130–134.
[21] T. Helgaker, T. A. Ruden, P. Jørgensen, J. Olsen, W. Klopper, *A priori* calculation of molecular properties to chemical accuracy, J. Phys. Org. Chem. 17 (11) (2004) 913–933.
[22] A. Yachmenev, S. N. Yurchenko, T. Ribeyre, W. Thiel, High-level *ab initio* potential energy surfaces and vibrational energies of H_2CS, J. Chem. Phys. 135 (2011) 074302.
[23] I. M. Mills, in: K. N. Rao, C. W. Mathews (Eds.), Molecular Spectroscopy - Modern Research, Academic Press, New York, 1972.
[24] J. K. G. Watson, in: J. R. During (Ed.), Vibrational Spectra and Structure, Elsevier, Amsterdam, 1977.
[25] D. Papousek, M. R. Aliev, Molecular Vibration-Rotation Spectra, Elsevier, Amsterdam, 1982.
[26] J. Breidung, H. Bürger, C. Kötting, R. Kopitzky, W. Sander, M. Senzlober, W. Thiel, H. Willner, Difluorovinyliden F_2C=C, Angew. Chem. Int. Ed. 36 (1997) 1983–1985.
[27] K. Aarset, A. G. Csàsàr, E. L. Sibert III, W. D. Allen, H. F. Schaefer III, W. Klopper, J. Noga, Anharmonic force field, vibrational energies, and barrier to inversion of SiH_3^-, J. Chem. Phys. 112 (9) (2000) 4053–4063.
[28] K. Diri, E. M. Myshakin, K. D. Jordan, On the contribution of vibrational anharmonicity to the binding energies of water clusters, J. Phys. Chem. A 109 (2005) 4005–4009.
[29] E. Cané, A. Miani, A. Trombetti, Anharmonic force fields of naphthalene-$h8$ and naphthalene-$d8$, J. Phys. Chem. A 111 (2007) 8218–8222.
[30] H. G. Kjaergaard, A. L. Gard, G. M. Chaban, R. B. Gerber, D. A. Matthews, J. F. Stanton, Calculation of vibrational transition frequencies and intensities in water dimer: Comparison of different vibrational approaches, J. Phys. Chem. A 112 (2008) 4324–4335.
[31] J. F. Stanton, B. A. Flowers, D. A. Matthews, A. F. Ware, G. B. Ellison, Gas-phase infrared spectrum of methyl nitrate, J. Molec. Spectrosc. 251 (2008) 384–393.
[32] C. J. Johnson, M. E. Harding, B. L. J. Poad, J. F. Stanton, R. E. Continetti, Electron affinities, well depths, and vibrational spectroscopy of *cis*- and *trans*-HOCO, J. Am. Chem. Soc. 133 (2011) 1960619609.
[33] R. C. Fortenberry, T. D. Crawford, T. J. Lee, The potential interstellar anion CH_2CN^-: Spectroscopic constants, vibrational frequencies, and other considerations, Astrophys. J. 762 (2013) 121.
[34] J. M. L. Martin, P. R. Taylor, Benchmark *ab initio* thermochemistry of the isomers of diimide, N_2H_2, using accurate computed structures and anharmonic force fields, Mol. Phys. 96 (4) (1999) 681–692.
[35] M. Torrent-Sucarrat, J. M. Luis, B. Kirtman, Variational calculation of vibrational linear and nonlinear optical properties, J. Chem. Phys. 122 (2005) 204108.
[36] D. W. Schwenke, Variational calculations of rovibrational energy levels and transition intensities for tetratomic molecules, J. Phys. Chem. 100 (1996) 2867–2884.
[37] M. Mladenović, Discrete variable approaches to tetratomic molecules: Part I: DVR(6) and DVR(3)+DGB methods, Spectrochim. Acta, Part A. 58 (4) (2002) 795–807.
[38] X. Huang, D. W. Schwenke, T. J. Lee, An accurate global potential energy surface, dipole moment surface, and rovibrational frequencies for NH_3, J. Chem. Phys. 129 (2008) 214304.
[39] X. Huang, D. W. Schwenke, T. J. Lee, Rovibrational spectra of ammonia. I. Unprecedented accuracy of a potential energy surface used with nonadiabatic corrections, J. Chem. Phys. 134 (2011) 044320.
[40] X. Huang, D. W. Schwenke, T. J. Lee, Rovibrational spectra of ammonia. II. Detailed analysis, comparison, and prediction of spectroscopic assignments for $^{14}NH_3$, $^{15}NH_3$, and $^{14}ND_3$, J. Chem. Phys. 134 (2011) 044321.
[41] M. Mladenović, Vibrational calculation for the HOCO radical and the *cis*-HOCO anion, J. Chem. Phys. 137 (2012) 014306.
[42] S. N. Yurchenko, W. Thiel, P. Jensen, Theoretical ROVibrational Energies (TROVE): a robust numerical approach to the calulation of rovibrational energies for polyatomic molecules, J. Molec. Spectrosc. 245 (2007) 126–140.
[43] S. N. Yurchenko, R. J. Barber, A. Yachmenev, W. Thiel, P. Jensen, J. Tennyson, A variationally computed T = 300 K line list for NH_3, J. Phys. Chem. A 113 (2009) 11845–11855.

[44] S. N. Yurchenko, R. J. Barber, J. Tennyson, W. Thiel, P. Jensen, Towards efficient refinement of molecular potential energy surfaces: Ammonia as a case study, J. Mol. Spectrosc. 268 (2011) 123–129.
[45] S. N. Yurchenko, A. Yachmenev, W. Thiel, O. Baum, T. F. Giesen, V. V. Melnikov, P. Jensen, An *ab initio* calculation of the vibrational energies and transition moments of HSOH, J. Molec. Spectrosc. 257 (2009) 57–65.
[46] A. Yachmenev, S. N. Yurchenko, P. Jensen, O. Baum, T. F. Giesen, W. Thiel, Theoretical rotation-torsion spectra of HSOH, Phys. Chem. Chem. Phys. 12 (2010) 8387–8397.
[47] S. Carter, J. M. Bowman, N. C. Handy, Extensions and tests of "Multimodes": a code to obtain accurate vibration/rotation energies of many-mode molecules, Theor. Chem. Acc. 100 (1-4) (1998) 191–198.
[48] J. M. Bowman, S. Carter, X. Huang, Multimode: a code to calculate rovibrational energies of polyatomic molecules, Int. Rev. Phys. Chem. 22 (3) (2003) 533–549.
[49] S. Carter, A. R. Sharma, J. M. Bowman, P. Rosmus, R. Tarroni, Calculations of rovibrational energies and dipole transition intensities for polyatomic molecules using multimode, J. Chem. Phys. 131 (2009) 224106.
[50] S. Carter, J. M. Bowman, N. C. Handy, Multimode calculations of rovibrational energies of C_2H_4 and C_2D_4, Mol. Phys. 110 (9-10) (2012) 775–781.
[51] J. K. G. Watson, Simplification of the molecular vibration-rotation Hamiltonian, Mol. Phys. 15 (1968) 479–486.
[52] R. Burcl, S. Carter, N. C. Handy, On the representation of potential energy surfaces of polayatomic molecules in normal coordinates: II. Parameterisation of the force field, Chem. Phys. Lett. 373 (2003) 357–365.
[53] O. Christiansen, Vibrational structure theory: new vibrational wave function methods for calculation of anharmonic vibrational energies and vibrational contributions to molecular properties, Phys. Chem. Chem. Phys. 9 (2007) 2942–2953.
[54] M. Keçeli, T. Shiozakia, K. Yagi, S. Hirata, Anharmonic vibrational frequencies and vibrationally-averaged structures of key species in Y−Y hydrocarbon combustion: HCO^+, HCO, HNO, HOO, HOO^-, CH_3, and CH_3, Mol. Phys. 107 (2009) 1283–1301.
[55] J. L. Dunham, The Wentzel-Brillouin-Kramers method of solving the wave equation, Phys. Rev. 41 (1932) 713–720.
[56] J. L. Dunham, The energy levels of a rotating vibrator, Phys. Rev. 41 (1932) 721–731.
[57] G. Simons, R. G. Parr, J. M. Finlan, New alternative to the Dunham potential for diatomic molecules, J. Chem. Phys. 59 (6) (1973) 3229–3234.
[58] W. Meyer, P. Botschwina, P. Burton, *ab initio* calculation of nearequilibrium potential and multipole moment surfaces and vibrational frequencies of $H_3{}^+$ and its isotopomers, J. Chem. Phys. 84 (1986) 891–900.
[59] S. Carter, N. C. Handy, A theoretical determination of the rovibrational energy levels of the water molecule, J. Chem. Phys. 87 (1987) 4294–4301.
[60] T. H. Dunning, Gaussian basis sets for use in correlated molecular calculations. I. The atoms boron through neon and hydrogen, J. Chem. Phys. 90 (1989) 1007–1023.
[61] D. E. Woon, T. H. Dunning, Gaussian basis sets for use in correlated molecular calculations. V. Core valence basis sets for boron through neon, J. Chem. Phys. 103 (1995) 4572–4585.
[62] R. A. Kendall, T. H. Dunning, R. J. Harrison, Electron affinities of the firstrow atoms revisited. Systematic basis sets and wave functions, J. Chem. Phys. 96 (1992) 6796–6806.
[63] J. M. L. Martin, T. J. Lee, The atomization energy and proton affinity of nh_3. an *ab initio* calibration study, Chem. Phys. Lett. 258 (1996) 136.
[64] D. L. Gray, A. G. Robiette, The anharmonic force field and equilibrium structure of methane, Mol. Phys. 37 (6) (1979) 1901–1920.
[65] A. P. Rendell, T. J. Lee, P. R. Taylor, Vibrational frequencies for Be_3 and Be_4, J. Chem. Phys. 92 (1990) 7050–7058.
[66] J. M. L. Martin, T. J. Lee, Accurate *ab initio* quartic force field and vibrational frequencies of the $NH_4{}^+$ ion and its deuterated forms, Chem. Phys. Lett. 258 (1996) 129–135.
[67] T. D. Crawford, S. S. Wesolewski, E. F. Valeev, R. A. King, M. L. Leininger, H. F. Schaefer, The past, present, and future of quantum chemistry, in: E. Keinan (Ed.), Chemistry in the 21st Century, Wiley, West Sussex, England, 2001.
[68] A. Szabo, N. S. Ostlund, Modern Quantum Chemistry: Introduction to Advanced Electronic Structure Theory, Dover, Mineola, NY, 1996.
[69] T. J. Lee, A. P. Rendell, K. G. Dyall, D. Jayatilaka, Open-shell restricted Hartree-Fock perturbation

theory: Some considerations and comparisons, J. Chem. Phys. 100 (1994) 7400–7409.
[70] L. O. Hargiss, W. C. Ermler, Vibrational-rotational analysis of *ab initio* potential energy surfaces for symmetric-top molecules: Application to ammonia isotopomers, J. Phys. Chem. 92 (1988) 300–306.
[71] J. M. L. Martin, T. J. Lee, Accurate ab initio quartic force fields for borane and BeH_2, Chem. Phys. Lett. 200 (5) (1992) 502–510.
[72] W. D. Allen, Y. Yamaguchi, A. G. Csàsàr, D. A. Clabo Jr., R. B. Remington, H. F. Schaefer III, A systematic study of molecular vibrational anharmonicity and vibration-rotation interaction by self-consistent-field higher-derivative methods. Linear polyatomic molecules, Chem. Phys. 145 (1990) 427–466.
[73] J. M. L. Martin, P. R. Taylor, T. J. Lee, Accurate *ab initio* quartic force fields for the ions HCO^+ and HOC^+, J. Chem. Phys. 99 (1993) 286–292.
[74] G. Strey, I. M. Mills, Anharmonic force field of acetylene, J. Molec. Spectrosc. 59 (1976) 103–113.
[75] J. M. L. Martin, T. J. Lee, P. R. Taylor, A purely *ab initio* spectroscopic quality quartic force field for acetylene, J. Chem. Phys. 108 (1998) 676–691.
[76] F. A. Cotton, Chemical Applications of Group Theory, 3rd Edition, Wiley, New York, 1990.
[77] J. Tennyson, N. F. Zobov, R. Williamson, O. L. Polyansky, P. F. Bernath, Experimental energy levels of the water molecule, J. Phys. Chem. Ref. Data 30 (3) (2003) 735–832.
[78] J. F. Gaw, A. Willets, W. H. Green, N. C. Handy, *SPECTRO program*, version 3.0, 1996.
[79] T. Rajamäki, A. Miani, L. Halonen, Vibrational energy levels for symmetric and asymmetric isotopomers of ammonia with an exact kinetic energy operator and new potential energy surfaces, J. Chem. Phys. 118 (14) (2003) 6358–6369.
[80] J. Demaison, L. Margulès, J. E. Boggs, Equilibrium structure and force field of NH_2, Phys. Chem. Chem. Phys. 5 (2003) 3359–3363.
[81] S. J. Blanksby, G. B. Ellison, Bond dissociation energies of organic molecules, Acc. Chem. Res. 36 (2003) 255–263.
[82] A. Owyung, C. W. Patterson, R. S. McDowell, CW stimulated Raman gain spectroscopy of the ν_1 fundamental of methane, Chem. Phys. Lett. 59 (1) (1978) 156–162.
[83] K. Kawaguchi, Fourier transform infrared spectroscopy of the BH_3 ν_2 band, Can. J. Phys. 72 (1994) 925–929.
[84] K. Kawaguchi, Fourier transform infrared spectroscopy of the BH_3 ν_3 band, J. Chem. Phys. 96 (1992) 3411–3415.

Figure 1: The 1-dimensional potential energy curves of the unrelaxed O−H stretch in water: Black is BLBA, blue is Morse-cosine with the 0.7 scale factor for α, red is Morse-cosine without α scaling, and green is Morse-cosine for 1.3 α. The black horizontal line is the O−H symmetric stretch fundamental for BLBA coordinates while red, slightly below, is the same but with unscaled α Morse-cosine coordinates.

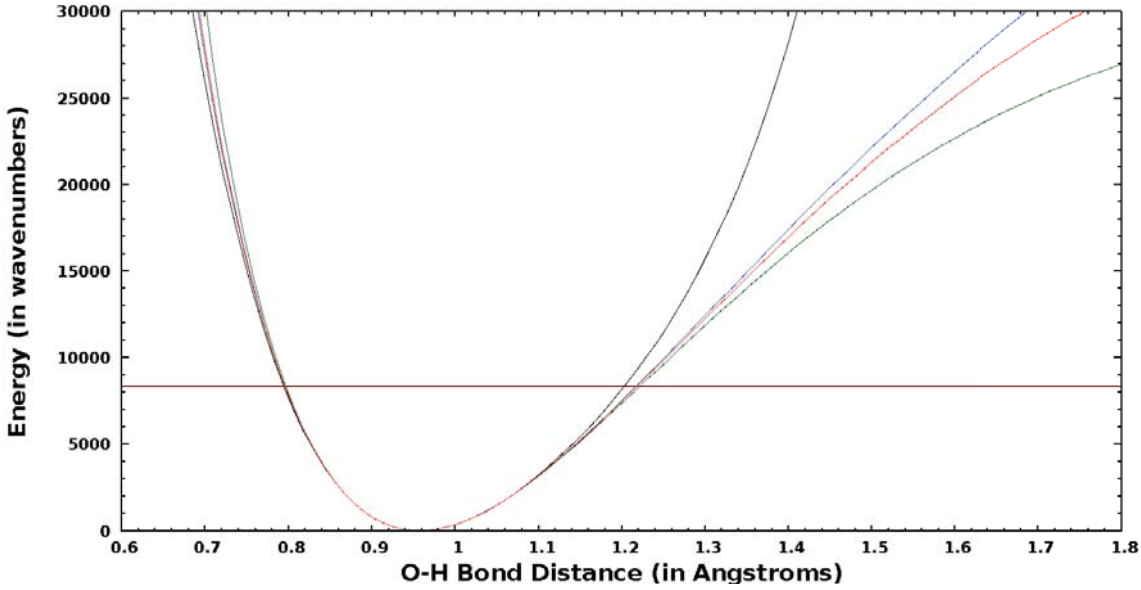

Table 1: Comparison between vibrational methods and coordinate systems for the fundamentals (in cm^{-1}) of NH_3.[a]

	mode	Morse-theta VTET	Morse-cosine VTET	Morse-cosine MM 6MR	Morse-cosine TROVE	HSL2[b] VTET	Non-adiabatic HSL2 VTET
A_1'	ν_1^+	3332.98	3333.09	3332.07	3332.32	3336.48	3336.10
A_2''	ν_1^-	3334.06	3334.13	3333.19	3333.38	3337.47	3337.08
A_1'	ν_2^+	927.10	928.80	928.94	928.65	932.64	932.44
A_2''	ν_2^-	964.31	965.67	965.32	965.45	968.43	968.16
A_2''	0^-	0.829	0.82	1.14	0.82	0.795	0.793
E'	ν_3^+	3440.86	3441.00	3440.21	3440.18	3444.04	3443.63
E''	ν_3^-	3441.21	3441.35	3440.92	3440.55	3444.40	3443.98
E'	ν_4^+	1623.75	1625.67	1625.20	1625.33	1626.75	1626.28
E''	ν_4^-	1624.89	1626.80	1626.70	1626.46	1627.85	1627.37

[a]Unless otherwise noted, all computations employ the QFF components of the HSL2 global PES from Refs. 39, 40.

[b]These computations were executed with the HSL2 global PES from Ref. 39, 40.

Figure 2: The 1-dimensional potential energy curves of the unrelaxed N−H stretch for ammonia: Black is, again, BLBA, blue is Morse-theta with the 0.7 α, red is Morse-cosine without α scaling, and green is Morse-cosine for 1.3 α.

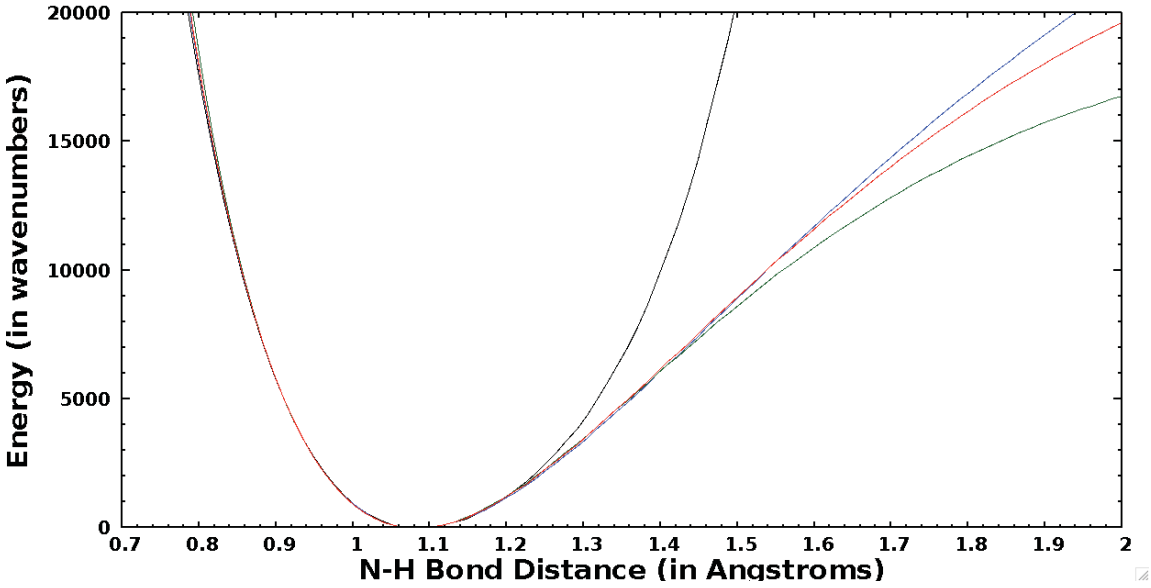

Figure 3: The 1-dimensional potential energy curves of a single unrelaxed C−H stretch in methane: Black is BLBA, blue is 0.7 α Morse-cosine, red is non-scaled Morse-cosine, and green is Morse-cosine for 1.3 α.

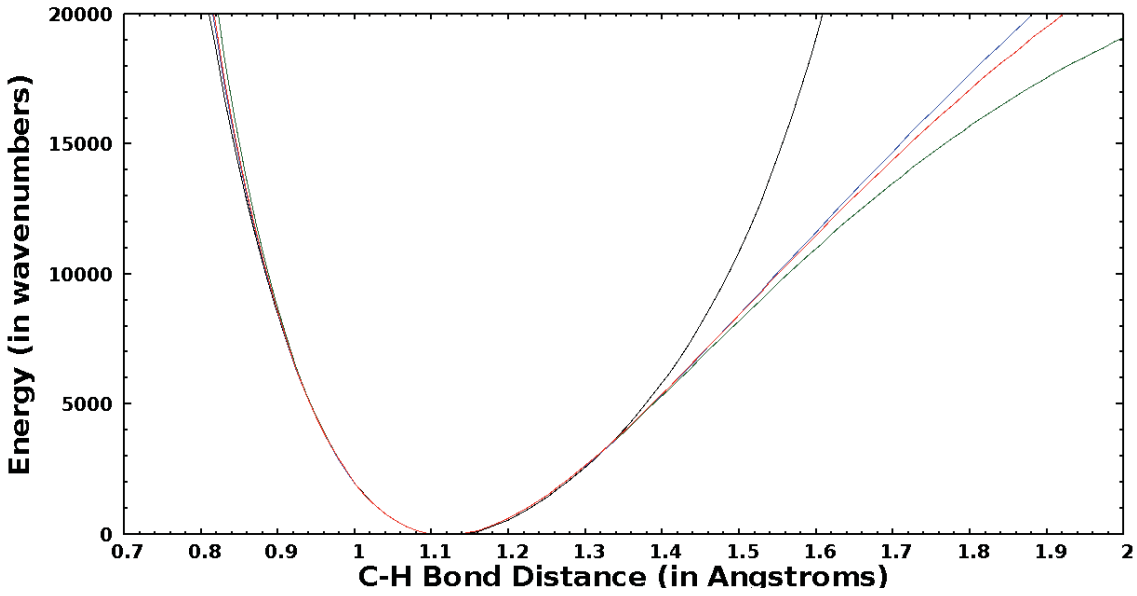

Figure 4: The 1-dimensional potential energy curves of the unrelaxed H−O−H bond angle for water: Black is BLBA, and red is from Morse-cosine coordinates.

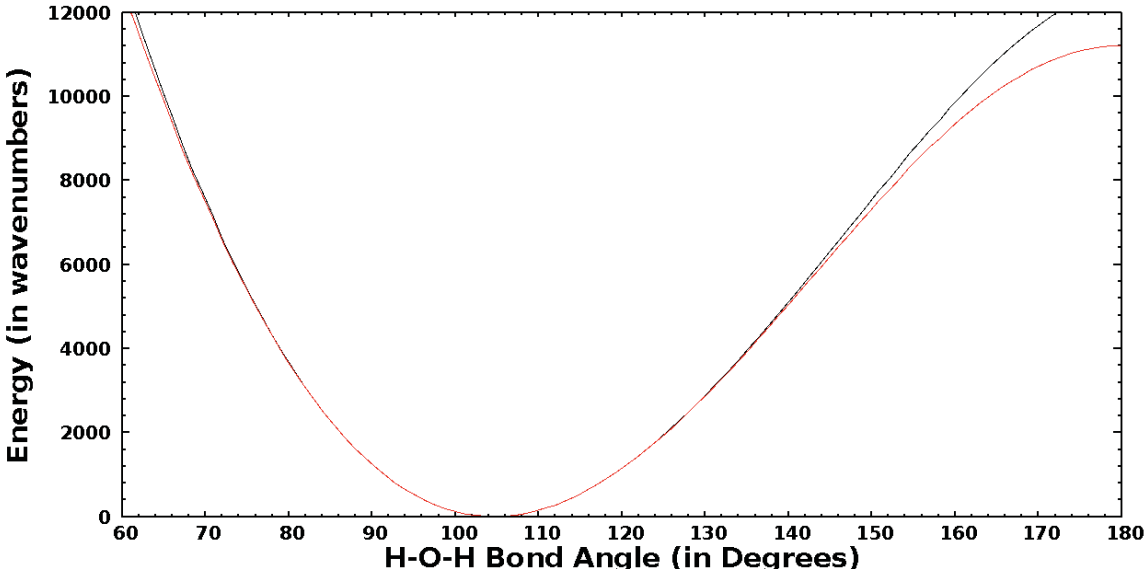

Table 2: Comparison of α scale factors for $\alpha = 2.15251489$ in Morse-theta coordinates for the TROVE fundamental frequencies and the bond dissociation energy (all in cm^{-1}) at equilibrium, D_e, for NH_3.

	mode	0.5	0.7	0.9	0.95	1.0	1.05	1.1	1.3	1.5	0.95-1.05	HSL2[a] VTET	Non-adiabatic HSL2 VTET[b]
A_1'	ν_1^+	3337.45	3335.53	3334.30	3333.83	3333.27	3332.59	3331.82	3327.79	3322.81	1.24	3336.48	3336.10
A_2''	ν_1^-	3338.57	3336.64	3335.41	3334.94	3334.37	3333.69	3332.92	3328.88	3323.88	1.25	3337.47	3337.08
A_1'	ν_2^+	928.32	928.22	928.01	927.96	927.93	927.90	927.89	928.08	928.84	0.06	932.64	932.44
A_2''	ν_2^-	965.42	965.30	965.14	965.10	965.06	965.02	964.99	964.94	965.11	0.08	968.43	968.16
A_2''	0^-	0.826	0.825	0.827	0.827	0.827	0.827	0.827	0.823	0.813	0.000	0.795	0.793
E'	ν_3^+	3445.82	3443.28	3441.55	3440.92	3440.18	3439.31	3438.32	3433.20	3426.79	1.61	3444.04	3443.63
E''	ν_3^-	3446.20	3443.66	3441.92	3441.30	3440.55	3439.68	3438.69	3433.58	3427.17	1.62	3444.40	3443.98
E'	ν_4^+	1625.36	1625.34	1625.33	1625.31	1625.28	1625.24	1625.18	1624.74	1623.93	0.07	1626.75	1626.28
E''	ν_4^-	1626.49	1626.47	1626.47	1626.45	1626.42	1626.37	1626.31	1625.87	1625.04	0.08	1627.85	1627.37
D_e		92487.9	56196.2	46027.2	43928.9	41924.4	40008.6	38179.8	31719.8	26525.7	3920.3		40520.0[c]
D_e/Exp. D_e[c]		228.25%	138.69%	113.59%	108.41%	103.47%	98.74%	94.22%	78.28%	65.46%	9.67%		

[a]VTET values here are computed with the HSL2 global PES from Ref. 39, 40.

[b]The non-adiabatic HSL2 VTET results already exhibit spectroscopic accuracy (as compared to vibrational frequencies collected in Ref. 79) and will function as the reference frequencies.

[c]The experimental D_e of 40520 cm^{-1} is derived from D_0 and the necessary vibrational frequencies from Ref. 80.

Table 3: Comparison of α for various scaling factors (α = 2.31348865) for the fundamentals and the dissociation energy (in cm^{-1}) of water using Morse-cosine coordinates with cC VCI.

	mode	0.5	0.7	0.9	0.95	1.0	1.05	1.1	1.3	1.5	0.95-1.05	VPT2	Reference[a]
ZPE		4645.53	4645.08	4644.82	4644.75	4644.68	4644.61	4644.57	4644.89	4646.94	0.14	4662.72	(4638.39)
Symmetric stretch	ν_1	3667.82	3665.22	3663.35	3662.67	3661.86	3660.93	3659.87	3654.66	3648.72	1.84	3662.53	3657.04
Bend	ν_2	1592.12	1592.06	1592.02	1592.00	1591.96	1591.90	1591.84	1591.36	1590.50	0.10	1594.54	1594.78
Antisymmetric stretch	ν_3	3767.02	3764.22	3762.18	3761.45	3760.58	3759.58	3758.44	3752.81	3746.24	1.87	3760.92	3755.96
D_e			57201.6	47324.5	45224.5	43204.5	41263.7	39403.7	32792.3		3960.8		44013.3[b]
D_e/Exp. D_e[b]			129.96%	107.52%	102.75%	98.16%	93.75%	89.53%	74.51%		9.00%		

[a]Reference data for H_2O fundamental vibrational frequencies from Ref. 77.

[b]The experimental D_e value is computed from the experimental D_0 and totally symmetric frequencies from Ref. 81.

Table 4: Comparison of scaled methane α values ($\alpha = 1.913958921$) for VCI 5MR LMT (from Ref. [4]) QFF Morse-cosine fundamentals and dissociation energies (in cm^{-1}).

	mode	0.5	0.7	0.9	0.95	1.0	1.05	1.1	1.3	1.5	0.95-1.05	VPT2	Reference[a]
ZPE		9738.14	9737.46	9737.05	9736.91	9736.77	9736.62	9736.48	9736.30	9737.79	0.29	9666.96	
A_1	ν_1	2920.29	2918.60	2917.30	2916.84	2916.31	2915.69	2915.00	2911.56	2907.55	1.15	2912.9	2916.5
E	ν_2	1532.59	1532.60	1532.63	1532.62	1532.60	1532.56	1532.51	1532.13	1531.32	0.06	1532.7	1533.3
T_2	ν_3	3021.84	3019.97	3018.65	3018.18	3017.60	3016.99	3016.26	3012.57	3008.14	1.19	3015.4	3019.2
T_2	ν_4	1312.94	1312.91	1312.89	1312.87	1312.85	1312.81	1312.76	1312.40	1311.68	0.06	1314.0	1310.8
D_e				44967.7	42818.1	40789.1	38867.5	37046.3			3950.6		39813.7[b]
D_e/Exp. D_e[b]				112.94%	107.54%	102.45%	97.62%	93.05%			9.92%		

[a]Reference data for CH_4 fundamental vibrational frequencies from Ref. 64 and Ref. 82 for ν_1.

[b]The experimental D_e value is computed from the experimental D_0 and totally symmetric frequencies from Ref. 81.

Table 5: Comparison of the NH_3 4MR, 5MR, and 6MR MM fundamental vibrational frequencies (in cm^{-1}).

Symmetry	Mode	4MR	5MR	6MR
A_1'	ν_1^+	3331.95	3332.06	3332.07
A_2''	ν_1^-	3332.99	3333.18	3333.19
A_1'	ν_2^+	928.13	929.06	928.94
A_2''	ν_2^-	963.98	965.47	965.32
A_2''	0^-	1.13	1.14	1.14
E'	ν_3^+	3439.20	3440.35	3440.21
E''	ν_3^-	3463.12	3440.94	3440.93
E'	ν_4^+	1619.74	1624.98	1625.20
E''	ν_4^-	1620.91	1626.48	1626.70

Table 6: Comparison of the CH_4 3MR, 4MR, and 5MR MM fundamental vibrational frequencies (in cm^{-1}).

Symmetry	Mode	3MR	4MR	5MR
A_1	ν_1	2915.08	2916.28	2916.41
E	ν_2	1532.56	1532.50	1532.63
		1532.76	1532.52	1532.63
T_2	ν_3	3018.87	3018.29	3017.97
		3027.82	3017.49	3018.10
		3027.82	3017.49	3018.10
T_2	ν_4	1312.69	1312.91	1313.04
		1312.66	1312.94	1313.04
		1312.66	1312.94	1313.04

Table 7: Comparison of the CBR[a] QFF BH_3 3MR, 4MR, 5MR, and 5MR-l[b] MM fundamental vibrational frequencies along with those from VPT2[c] and experiment (in cm^{-1}).

Symmetry	Mode	3MR	4MR	5MR	5MR-l[b]	VPT2[c]	Expt.[d]
A_1	ν_1	2500.4673	2500.9143	2500.9318	2500.8695	2502.3	
A_1	ν_2	1145.5123	1145.5366	1145.5444	1145.5445	1147.2	1147.4986
E'	ν_3	2602.8146	2602.8933	2602.9349	2602.8806	2602.1	2601.5743
		2606.8095	2602.8471	2602.9348	2602.8771		
E'	ν_4	1196.6687	1196.6686	1196.6889	1196.6059	1196.5	1196.66
		1196.5841	1196.6734	1196.6936	1196.6071		

[a]The CBR QFF is from Ref. 7 and is the CBS extrapolated, Born-Oppenheimer corrected, scalar relativistic QFF.
[b]The "-l" indicates that these 5MR results are using a basis set with more than twice as many functions.
[c]The VPT2 computations are from Ref. 7.
[d]The experimental ν_2 and ν_4 frequencies are from Ref. 83 with ν_3 from Ref. 84.

Table 8: H_2O fundamentals and first few overtones and combination bands from cC VPT2, cC 3MR (full-CI) VCI, experiment, and the differences from experiment for VPT2 and VCI (all in cm^{-1}).

Mode	VPT2	VCI	Exp.[a]	Exp. − VPT2	Exp. − VCI
ZPE	4662.72	4644.68	4638.39	24.33	6.29
ν_2	1594.54	1591.96	1594.746	0.21	2.79
$2\nu_2$	3153.87	3143.32	3151.630	-2.24	8.31
ν_1	3662.53	3661.86	3657.053	-5.48	-4.81
ν_3	3760.92	3760.58	3755.929	-4.99	-4.65
$3\nu_2$	4677.98	4649.42	4666.790	-11.19	17.37
$\nu_1 + \nu_2$	5240.84	5236.83	5234.978	-5.86	-1.85
$\nu_2 + \nu_3$	5335.68	5334.04	5331.265	-4.41	-2.77
$\nu_1 + 2\nu_2$	6783.92	6770.35	6775.093	-8.83	4.74
$2\nu_2 + \nu_3$	6875.22	6868.94	6871.520	-3.70	2.58
$2\nu_1$	7237.83	7205.20	7201.540	-36.29	-3.66
$\nu_1 + \nu_3$	7254.98	7251.97	7249.818	-5.16	-2.15
$2\nu_3$	7423.49	7453.23	7445.045	21.56	-8.18
$2\nu_1 + \nu_2$	8799.90	8763.69	8761.582	-38.32	-2.11
$\nu_1 + \nu_2 + \nu_3$	–	8809.05	8806.999	–	-2.05
$\nu_2 + 2\nu_3$	8978.46	9008.41	9000.136	21.68	-8.27
$3\nu_1$	–	10596.39	10599.686	–	3.30

[a] Reference 77.